

Electromagnetic scattering by homogeneous, isotropic, dielectric-magnetic sphere with topologically insulating surface states

Akhlesh Lakhtakia

The Pennsylvania State University, Department of Engineering Science and Mechanics, Nanoengineered Metamaterials Group, University Park, PA 16802, USA

Tom G. Mackay

The Pennsylvania State University, Department of Engineering Science and Mechanics, Nanoengineered Metamaterials Group, University Park, PA 16802, USA

]University of Edinburgh, School of Mathematics and Maxwell Institute for Mathematical Sciences, Edinburgh EH9 3FD, Scotland, United Kingdom

Abstract

The Lorenz–Mie formulation of electromagnetic scattering by a homogeneous, isotropic, dielectric-magnetic sphere was extended to incorporate topologically insulating surface states characterized by a surface admittance γ . Closed-form expressions were derived for the expansion coefficients of the scattered field phasors in terms of those of the incident field phasors. These expansion coefficients were used to obtain analytical expressions for the total scattering, extinction, forward scattering, and backscattering efficiencies of the sphere. Resonances exist for relatively low values of γ , when the sphere is either nondissipative or weakly dissipative. For large values of γ , the scattering characteristics are close to that of a perfect electrically conducting sphere, regardless of whether the sphere is composed of a dissipative or nondissipative material, and regardless of whether that material supports planewave propagation with positive or negative phase velocity.

1 Introduction

Complete analytical treatment of electromagnetic planewave scattering by a homogeneous, isotropic, dielectric sphere [1] can be traced back to an 1890 paper of Lorenz [2, 3], though credit for that achievement is commonly given to a 1908 paper of Mie [4]. The incident, the scattered, and the internal fields are expanded as series of vector spherical wavefunctions [5, 6], the surface of the sphere is taken to be charge free and current free, the standard boundary conditions of electromagnetics are imposed, and the orthogonality properties of the trigonometric functions and the associated Legendre functions are exploited. Extensions of this treatment to isotropic dielectric-magnetic spheres [5, 7], bi-isotropic spheres [8], and some orthorhombic dielectric-magnetic spheres [9, 10] have been reported.

Electrification of the surfaces of dielectric particles is commonly observed [11, 12, 13]. It too can be incorporated in the Lorenz–Mie formulation through a two-sided boundary condition involving a surface electric current density that is proportional to the tangential electric field [14]. This type of impedance boundary condition is the same as commonly used for carbon nanotubes [15] and represents the formation of surface states for electronic propagation [15, 16, 17].

Surface states exist on topological insulators as protected conducting states and are responsible for the characteristic electromagnetic responses of these materials [18]. Two classical-electromagnetic models have been proposed for these materials as follows.

- I. The topological insulator is an achiral nonreciprocal bi-isotropic material characterized by three scalar constitutive parameters: the relative permittivity ϵ_r , the relative permeability μ_r , and the Tellegen nonreciprocity parameter γ [19]. The surface of a finite region occupied by the topological insulator is charge-neutral and current-neutral.
- II. The topological insulator is an isotropic dielectric-magnetic material characterized by the relative permittivity ϵ_r and the relative permeability μ_r , but its surface is endowed with surface charge and current densities quantitated through a non-null surface admittance γ [20].

Model I is physically inadequate because the essential macroscopic physics of topological insulation occurs not inside a region but on the surface of that region. Indeed, the Tellegen nonreciprocity parameter disappears

from the Maxwell equations applicable to that region [21], and even leads by itself to a contradiction [22]. In contrast, the surface admittance of Model II appears in the boundary conditions, in consonance with the existence of *surface* states. Let us note, in passing, that any model of a topological insulator with $\gamma = 0$ and a surface conductivity derivable from a complex relative permittivity [23] ignores the existence of surface states, and therefore should be valid only under the long-wavelength approximation.

In this paper, we adopt Model II to extend the Lorenz–Mie formulation in order to encompass electromagnetic scattering by a homogeneous, isotropic, dielectric-magnetic sphere with topologically insulating surface states. The incident field is not necessarily a plane wave, but its sources must lie outside the sphere [24, 25] and are assumed to be unaffected by the scattered field. The $\exp(-i\omega t)$ time dependence is implicit, with $i = \sqrt{-1}$, ω as the angular frequency, and t as time. The free-space wavenumber $k_0 = \omega\sqrt{\varepsilon_0\mu_0}$ and the free-space intrinsic impedance $\eta_0 = \sqrt{\mu_0/\varepsilon_0}$, where ε_0 and μ_0 are the permittivity and permeability of free space, respectively. Vector quantities are displayed in bold typeface, with the superscript symbol $\hat{}$ denoting a unit vector.

2 Boundary-value problem

Consider the sphere $r < a$ made of an isotropic dielectric-magnetic material with relative permittivity ε_r and relative permeability μ_r . We also define a surface admittance γ for use in boundary conditions at $r = a$, in accordance with the physically appropriate Model II. The external region $r > a$ is vacuous.

2.1 Incident electromagnetic field

In a region that completely encloses the spherical surface $r = a$ but excludes the sources of the incident electromagnetic field, the incident electric and magnetic field phasors are represented as [24, 25]

$$\mathbf{E}_{\text{inc}}(\mathbf{r}) = \sum_{s \in \{e, o\}} \sum_{n=1}^{\infty} \sum_{m=0}^n \left\{ D_{mn} \left[A_{\text{smn}}^{(1)} \mathbf{M}_{\text{smn}}^{(1)}(k_0 \mathbf{r}) + B_{\text{smn}}^{(1)} \mathbf{N}_{\text{smn}}^{(1)}(k_0 \mathbf{r}) \right] \right\}, \quad (1)$$

$$\mathbf{B}_{\text{inc}}(\mathbf{r}) = \frac{k_0}{i\omega} \sum_{s \in \{e, o\}} \sum_{n=1}^{\infty} \sum_{m=0}^n \left\{ D_{mn} \left[A_{\text{smn}}^{(1)} \mathbf{N}_{\text{smn}}^{(1)}(k_0 \mathbf{r}) + B_{\text{smn}}^{(1)} \mathbf{M}_{\text{smn}}^{(1)}(k_0 \mathbf{r}) \right] \right\}, \quad (2)$$

where the vector spherical wavefunctions $\mathbf{M}_{\text{smn}}^{(1)}(k_0 \mathbf{r})$ and $\mathbf{N}_{\text{smn}}^{(1)}(k_0 \mathbf{r})$ [5, 6] are defined in the Appendix, and the normalization factor

$$D_{mn} = (2 - \delta_{m0}) \frac{(2n+1)(n-m)!}{4n(n+1)(n+m)!} \quad (3)$$

employs the Kronecker delta $\delta_{mm'}$. The coefficients $A_{\text{smn}}^{(1)}$ and $B_{\text{smn}}^{(1)}$ are presumed to be known. The functions $\mathbf{M}_{\text{smn}}^{(1)}(k_0 \mathbf{r})$ are classified as toroidal and the functions $\mathbf{N}_{\text{smn}}^{(1)}(k_0 \mathbf{r})$ as poloidal [26].

2.2 Scattered electromagnetic field

The scattered electric and magnetic field phasors are represented as [27, 28]

$$\mathbf{E}_{\text{sca}}(\mathbf{r}) = \sum_{s \in \{e, o\}} \sum_{n=1}^{\infty} \sum_{m=0}^n \left\{ D_{mn} \left[A_{\text{smn}}^{(3)} \mathbf{M}_{\text{smn}}^{(3)}(k_0 \mathbf{r}) + B_{\text{smn}}^{(3)} \mathbf{N}_{\text{smn}}^{(3)}(k_0 \mathbf{r}) \right] \right\}, \quad r > a, \quad (4)$$

$$\mathbf{B}_{\text{sca}}(\mathbf{r}) = \frac{k_0}{i\omega} \sum_{s \in \{e, o\}} \sum_{n=1}^{\infty} \sum_{m=0}^n \left\{ D_{mn} \left[A_{\text{smn}}^{(3)} \mathbf{N}_{\text{smn}}^{(3)}(k_0 \mathbf{r}) + B_{\text{smn}}^{(3)} \mathbf{M}_{\text{smn}}^{(3)}(k_0 \mathbf{r}) \right] \right\}, \quad r > a, \quad (5)$$

where the vector spherical wavefunctions $\mathbf{M}_{\text{smn}}^{(3)}(k_0 \mathbf{r})$ and $\mathbf{N}_{\text{smn}}^{(3)}(k_0 \mathbf{r})$ [5, 6] are defined in the Appendix. The coefficients $A_{\text{smn}}^{(3)}$ and $B_{\text{smn}}^{(3)}$ have to be determined. The functions $\mathbf{M}_{\text{smn}}^{(3)}(k_0 \mathbf{r})$ are classified as toroidal and the functions $\mathbf{N}_{\text{smn}}^{(3)}(k_0 \mathbf{r})$ as poloidal.

In the far zone, the scattered electric field may be approximated as [29]

$$\mathbf{E}_{\text{sca}}(\mathbf{r}) \approx \mathbf{F}_{\text{sca}}(\theta, \phi) \frac{\exp(ik_0 r)}{r} \quad (6)$$

and the scattered magnetic field as

$$\mathbf{B}_{\text{sca}}(\mathbf{r}) \approx \frac{k_0}{\omega} \hat{\mathbf{r}} \times \mathbf{F}_{\text{sca}}(\theta, \phi) \frac{\exp(ik_0 r)}{r}, \quad (7)$$

where $\hat{\mathbf{r}} = \mathbf{r}/r$ and

$$\mathbf{F}_{\text{sca}}(\theta, \phi) = k_0^{-1} \sum_{s \in \{e, o\}} \sum_{n=1}^{\infty} \sum_{m=0}^n \left\{ (-i)^n D_{mn} \sqrt{n(n+1)} \left[-iA_{\text{smn}}^{(3)} \mathbf{C}_{\text{smn}}(\theta, \phi) + B_{\text{smn}}^{(3)} \mathbf{B}_{\text{smn}}(\theta, \phi) \right] \right\} \quad (8)$$

is the vector far-field scattering amplitude. The angular harmonics $\mathbf{B}_{\text{smn}}(\theta, \phi)$ and $\mathbf{C}_{\text{smn}}(\theta, \phi)$ [6] are defined in the Appendix.

2.3 Internal electromagnetic field

The electric and magnetic field phasors excited inside the chosen sphere are represented by [28]

$$\mathbf{E}_{\text{exc}}(\mathbf{r}) = \sum_{s \in \{e, o\}} \sum_{n=1}^{\infty} \sum_{m=0}^n \left\{ D_{mn} \left[\alpha_{\text{smn}} \mathbf{M}_{\text{smn}}^{(1)}(k\mathbf{r}) + \beta_{\text{smn}} \mathbf{N}_{\text{smn}}^{(1)}(k\mathbf{r}) \right] \right\}, \quad r < a, \quad (9)$$

$$\mathbf{B}_{\text{exc}}(\mathbf{r}) = \frac{k}{i\omega} \sum_{s \in \{e, o\}} \sum_{n=1}^{\infty} \sum_{m=0}^n \left\{ D_{mn} \left[\alpha_{\text{smn}} \mathbf{N}_{\text{smn}}^{(1)}(k\mathbf{r}) + \beta_{\text{smn}} \mathbf{M}_{\text{smn}}^{(1)}(k\mathbf{r}) \right] \right\}, \quad r < a, \quad (10)$$

the coefficients α_{smn} and β_{smn} being unknown. The wavenumber $k = \tilde{n}k_0$, where $\tilde{n} = \sqrt{\varepsilon_r \mu_r}$ is the refractive index. Equations (9) and (10) are respectively similar to Eqs. (1) and (2), because the source-free region $r < a$ contains the origin.

2.4 Boundary conditions

In accordance with Model II, the boundary conditions appropriate for a topological insulator are as follows:

$$\left. \begin{aligned} \hat{\mathbf{r}} \times [\mathbf{E}_{\text{inc}}(\mathbf{r}) + \mathbf{E}_{\text{sca}}(\mathbf{r}) - \mathbf{E}_{\text{exc}}(\mathbf{r})] &= \mathbf{0} \\ \hat{\mathbf{r}} \times \left\{ \mu_0^{-1} [\mathbf{B}_{\text{inc}}(\mathbf{r}) + \mathbf{B}_{\text{sca}}(\mathbf{r})] - (\mu_0 \mu_r)^{-1} \mathbf{B}_{\text{exc}}(\mathbf{r}) \right\} & \\ = -\gamma \hat{\mathbf{r}} \times \mathbf{E}_{\text{exc}}(\mathbf{r}) & \end{aligned} \right\},$$

$$r = a.$$
(11)

The surface admittance γ characterizing the topologically insulating surface states is very likely dependent on the free-space wavenumber as well as the constitution of the topological insulator, and it may also vary on the surface according to the local geometry. We hypothesize that a minimum radius of curvature is necessary for the existence of a non-null admittance. For a homogeneous sphere, symmetry suggests that the surface admittance does not vary on the surface. Furthermore, we expect that $\gamma = 0$ in the long-wavelength approximation ($k_0 a \ll 1$ and $|k|a \ll 1$ [30]) because surface states will be either non-existent or inconsequential in the absence of a sufficient volume. This expectation is in accord with experimental results [23] on very thin films of the topologically insulating chalcogenide Bi_2Se_3 , those experimental results being evidently accounted for by a surface conductivity arising from a permittivity, without requiring $\gamma \neq 0$.

The boundary conditions (11) differ from their counterparts [14]

$$\left. \begin{aligned} \hat{\mathbf{r}} \times [\mathbf{E}_{\text{inc}}(\mathbf{r}) + \mathbf{E}_{\text{sca}}(\mathbf{r}) - \mathbf{E}_{\text{exc}}(\mathbf{r})] &= \mathbf{0} \\ \hat{\mathbf{r}} \times \left\{ \mu_0^{-1} [\mathbf{B}_{\text{inc}}(\mathbf{r}) + \mathbf{B}_{\text{sca}}(\mathbf{r})] - (\mu_0 \mu_r)^{-1} \mathbf{B}_{\text{exc}}(\mathbf{r}) \right\} & \\ = \tilde{\sigma} (\underline{\underline{\mathbf{I}}} - \hat{\mathbf{r}}\hat{\mathbf{r}}) \cdot \mathbf{E}_{\text{exc}}(\mathbf{r}) & \end{aligned} \right\},$$

$$r = a,$$
(12)

that prevail on the surface of a charged sphere, where $\underline{\underline{\mathbf{I}}}$ is the identity dyadic [31] and the frequency-dependent surface conductivity $\tilde{\sigma}$ incorporates the charging of the surface $r = a$. The difference can be appreciated by noting that $\hat{\mathbf{r}} \times \mathbf{A} \neq (\underline{\underline{\mathbf{I}}} - \hat{\mathbf{r}}\hat{\mathbf{r}}) \cdot \mathbf{A}$ for an arbitrary vector $\mathbf{A} = A_r \hat{\mathbf{r}} + A_\theta \hat{\boldsymbol{\theta}} + A_\phi \hat{\boldsymbol{\phi}}$; indeed, $\hat{\mathbf{r}} \times \mathbf{A} = -\hat{\boldsymbol{\theta}} A_\phi + \hat{\boldsymbol{\phi}} A_\theta$ but $(\underline{\underline{\mathbf{I}}} - \hat{\mathbf{r}}\hat{\mathbf{r}}) \cdot \mathbf{A} = \hat{\boldsymbol{\theta}} A_\theta + \hat{\boldsymbol{\phi}} A_\phi$ on the surface of the sphere. The use of Eqs. (12) in lieu of Eqs. (11) is inadmissible for a topological insulator, as is clear from Sec. 22.7.

The twin boundary conditions (11) also differ from the sole boundary condition [32, 33]

$$\begin{aligned} \tilde{\sigma} \hat{\mathbf{r}} \times [\mathbf{E}_{\text{inc}}(\mathbf{r}) + \mathbf{E}_{\text{sca}}(\mathbf{r})] &= \\ -\mu_0^{-1} (\underline{\underline{\mathbf{I}}} - \hat{\mathbf{r}}\hat{\mathbf{r}}) \cdot [\mathbf{B}_{\text{inc}}(\mathbf{r}) + \mathbf{B}_{\text{sca}}(\mathbf{r})], & \quad r = a, \end{aligned}$$
(13)

that is taken to prevail on the surface of an impedance sphere. On taking the cross product of both sides with $\hat{\mathbf{r}}$, the boundary condition (13) is equivalently written as

$$\begin{aligned} \tilde{\sigma} (\underline{\underline{\mathbf{I}}} - \hat{\mathbf{r}}\hat{\mathbf{r}}) \cdot [\mathbf{E}_{\text{inc}}(\mathbf{r}) + \mathbf{E}_{\text{sca}}(\mathbf{r})] &= \\ \mu_0^{-1} \hat{\mathbf{r}} \times [\mathbf{B}_{\text{inc}}(\mathbf{r}) + \mathbf{B}_{\text{sca}}(\mathbf{r})], & \quad r = a. \end{aligned}$$
(14)

The use of an impedance boundary condition results in loss of information about the internal fields $\mathbf{E}_{\text{exc}}(\mathbf{r})$ and $\mathbf{B}_{\text{exc}}(\mathbf{r})$, and is generally adopted for perfectly conducting objects with somewhat rough [34] or coated surfaces [35]. An impedance boundary condition cannot represent the surface states of a topological insulator as becomes clear in Sec. 22.8.

2.5 Solution of boundary-value problem

After substituting Eqs. (1), (4), and (9) in Eq. (11)₁, and after exploiting the orthogonality properties of the trigonometric functions over $0 \leq \phi \leq 2\pi$ and of the associated Legendre functions over $0 \leq \theta \leq \pi$, we obtain

the simple algebraic equations

$$\left. \begin{aligned} A_{\text{smn}}^{(1)} j_n(\xi) + A_{\text{smn}}^{(3)} h_n^{(1)}(\xi) &= \alpha_{\text{smn}} j_n(\tilde{n}\xi) \\ \tilde{n} \left[B_{\text{smn}}^{(1)} \psi_n^{(1)}(\xi) + B_{\text{smn}}^{(3)} \psi_n^{(3)}(\xi) \right] &= \beta_{\text{smn}} \psi_n^{(1)}(\tilde{n}\xi) \end{aligned} \right\}, \quad (15)$$

where $\xi = k_0 a$. Likewise, after substituting Eqs. (2), (5), (9), and (10) in Eq. (11)₂, and after exploiting the orthogonality properties of the trigonometric functions over $0 \leq \phi \leq 2\pi$ and of the associated Legendre functions over $0 \leq \theta \leq \pi$, we obtain the following simple algebraic equations:

$$\left. \begin{aligned} \mu_r \left[A_{\text{smn}}^{(1)} \psi_n^{(1)}(\xi) + A_{\text{smn}}^{(3)} \psi_n^{(3)}(\xi) \right] \\ = [\alpha_{\text{smn}} - i(\eta_0 \gamma \tilde{n} / \varepsilon_r) \beta_{\text{smn}}] \psi_n^{(1)}(\tilde{n}\xi) \\ \frac{\tilde{n}}{\varepsilon_r} \left[B_{\text{smn}}^{(1)} j_n(\xi) + B_{\text{smn}}^{(3)} h_n^{(1)}(\xi) \right] \\ = [\beta_{\text{smn}} - i(\eta_0 \gamma \tilde{n} / \varepsilon_r) \alpha_{\text{smn}}] j_n(\tilde{n}\xi) \end{aligned} \right\}. \quad (16)$$

Equations (15) and (16) are straightforward to solve for $A_{\text{smn}}^{(3)}$, $B_{\text{smn}}^{(3)}$, α_{smn} , and β_{smn} in terms of $A_{\text{smn}}^{(1)}$ and $B_{\text{smn}}^{(1)}$. As our interest lies in the scattered fields, we are content to state that

$$\left. \begin{aligned} A_{\text{smn}}^{(3)} &= c_n A_{\text{smn}}^{(1)} + d_n B_{\text{smn}}^{(1)} \\ B_{\text{smn}}^{(3)} &= -d_n A_{\text{smn}}^{(1)} + e_n B_{\text{smn}}^{(1)} \end{aligned} \right\}, \quad (17)$$

where

$$\begin{aligned} \Delta_n c_n &= -s_n q_n \\ &+ (\eta_0 \gamma)^2 \mu_r j_n(\xi) \psi_n^{(3)}(\xi) j_n(\tilde{n}\xi) \psi_n^{(1)}(\tilde{n}\xi), \end{aligned} \quad (18)$$

$$\Delta_n d_n = (\eta_0 \gamma \mu_r / \xi) j_n(\tilde{n}\xi) \psi_n^{(1)}(\tilde{n}\xi), \quad (19)$$

$$\begin{aligned} \Delta_n e_n &= -p_n t_n \\ &+ (\eta_0 \gamma)^2 \mu_r h_n^{(1)}(\xi) \psi_n^{(1)}(\xi) j_n(\tilde{n}\xi) \psi_n^{(1)}(\tilde{n}\xi), \end{aligned} \quad (20)$$

$$\begin{aligned} \Delta_n &= q_n t_n \\ &- (\eta_0 \gamma)^2 \mu_r h_n^{(1)}(\xi) \psi_n^{(3)}(\xi) j_n(\tilde{n}\xi) \psi_n^{(1)}(\tilde{n}\xi), \end{aligned} \quad (21)$$

$$p_n = \varepsilon_r j_n(\tilde{n}\xi) \psi_n^{(1)}(\xi) - j_n(\xi) \psi_n^{(1)}(\tilde{n}\xi), \quad (22)$$

$$q_n = \varepsilon_r j_n(\tilde{n}\xi) \psi_n^{(3)}(\xi) - h_n^{(1)}(\xi) \psi_n^{(1)}(\tilde{n}\xi), \quad (23)$$

$$s_n = \mu_r j_n(\tilde{n}\xi) \psi_n^{(1)}(\xi) - j_n(\xi) \psi_n^{(1)}(\tilde{n}\xi), \quad (24)$$

$$t_n = \mu_r j_n(\tilde{n}\xi) \psi_n^{(3)}(\xi) - h_n^{(1)}(\xi) \psi_n^{(1)}(\tilde{n}\xi). \quad (25)$$

Toroidal-poloidal mixing on scattering is signified by $d_n \neq 0$.

2.6 Comparison with Model I

Planewave scattering by a homogeneous, isotropic, dielectric-magnetic sphere with topologically insulating surface states was solved by Ge *et al.* [36] recently using Model I. However, that boundary-value problem is a simple specialization of a more general one for a bi-isotropic sphere, solved four decades earlier by Bohren [8]. The specialization requires setting $\alpha + \beta = 0$ in Ref. [8].

Anyhow, we have verified that application of Model I also yields Eqs. (17)–(25). That both Models I and II yield the same electromagnetic field scattered by a finite region occupied by a topological insulator has been also noted for the planewave reflection and refraction due to a half space occupied by a homogeneous, isotropic, dielectric-magnetic material with topologically insulating surface states [37]. Thus, the two models lead to different boundary-value problems for scattering by a finite region occupied by a topological insulator, but the scattered field remains the same. This conclusion, however, does not affect the physical deficiency inherent in Model I, because surface states reside on a surface (and can therefore impact the boundary conditions through a surface admittance) whereas the Tellegen nonreciprocity parameter is a constitutive parameter that must hold in a region bounded by that surface. The experimental results of Autore *et al.* [23] clearly show that surface states vanish when the volume is very tiny, but a constitutive parameter has to be valid regardless of the volume.

2.7 Comparison with charged sphere

For a charged sphere [14], Eqs. (12) have to be used in lieu of Eqs. (11) but the remainder of the analytical treatment remains the same. As a result, for use in Eq. (17) the following expressions are obtained:

$$c_n = -\frac{i\eta_0\tilde{\sigma}\mu_r\xi j_n(\xi)j_n(\tilde{n}\xi) + s_n}{i\eta_0\tilde{\sigma}\mu_r\xi h_n^{(1)}(\xi)j_n(\tilde{n}\xi) + t_n}, \quad (26)$$

$$d_n = 0, \quad (27)$$

$$e_n = -\frac{i\eta_0\tilde{\sigma}\psi_n^{(1)}(\xi)\psi_n^{(1)}(\tilde{n}\xi) + \xi p_n}{i\eta_0\tilde{\sigma}\psi_n^{(3)}(\xi)\psi_n^{(1)}(\tilde{n}\xi) + \xi q_n}. \quad (28)$$

Clearly, toroidal-poloidal mixing does not occur on scattering by a charged sphere—unlike for an isotropic dielectric-magnetic sphere with topologically insulating surface states. Hence, a surface-conductivity model [23] is inadmissible for a dielectric-magnetic sphere with topologically insulating surface states.

2.8 Comparison with impedance sphere

For an impedance sphere [34, 35], either Eq. (13) or Eq. (14) has to be used in lieu of Eqs. (11), and the analytical treatment is similar. As a result, for use in Eq. (17) the following expressions are obtained:

$$c_n = -\frac{i\eta_0\tilde{\sigma}\xi j_n(\xi) + \psi_n^{(1)}(\xi)}{i\eta_0\tilde{\sigma}\xi h_n^{(1)}(\xi) + \psi_n^{(3)}(\xi)}, \quad (29)$$

$$d_n = 0, \quad (30)$$

$$e_n = -\frac{i\eta_0\tilde{\sigma}\psi_n^{(1)}(\xi) - \xi j_n(\xi)}{i\eta_0\tilde{\sigma}\psi_n^{(3)}(\xi) - \xi h_n^{(1)}(\xi)}. \quad (31)$$

Thus, as toroidal-poloidal mixing does not occur on scattering by an impedance sphere, an impedance boundary condition is inadmissible for a dielectric-magnetic sphere with topologically insulating surface states.

2.9 Comparison with perfect electrically conducting sphere

For a perfect electrically conducting (PEC) sphere [39], the limit $\tilde{\sigma} \rightarrow \infty$ must be taken in Eqs. (29)–(31) to obtain

$$c_n = -\frac{j_n(\xi)}{h_n^{(1)}(\xi)}, \quad (32)$$

$$d_n = 0, \quad (33)$$

$$e_n = -\frac{\psi_n^{(1)}(\xi)}{\psi_n^{(3)}(\xi)}. \quad (34)$$

2.10 Planewave scattering

Suppose that the incident electromagnetic field is a plane wave. Without loss of generality, we can take it to be traveling along the $+z$ axis; hence,

$$\left. \begin{aligned} \mathbf{E}_{\text{inc}}(\mathbf{r}) &= \hat{\mathbf{x}} \exp(ik_0 z) \\ \mathbf{B}_{\text{inc}}(\mathbf{r}) &= \frac{k_0}{\omega} \hat{\mathbf{y}} \exp(ik_0 z) \end{aligned} \right\}, \quad (35)$$

so that [5, 6, 27]

$$\left. \begin{aligned} A_{\text{smn}}^{(1)} &= 2n(n+1)i^n \delta_{so} \delta_{m1} \\ B_{\text{smn}}^{(1)} &= 2n(n+1)i^{n-1} \delta_{se} \delta_{m1} \end{aligned} \right\}. \quad (36)$$

Accordingly, the non-zero coefficients in the expansions of the scattered electric and magnetic fields are as follows:

$$\left. \begin{aligned} A_{o1n}^{(3)} &= c_n A_{o1n}^{(1)} \\ A_{e1n}^{(3)} &= d_n B_{e1n}^{(1)} \\ B_{o1n}^{(3)} &= -d_n A_{o1n}^{(1)} \\ B_{e1n}^{(3)} &= e_n B_{e1n}^{(1)} \end{aligned} \right\}. \quad (37)$$

Using these coefficients in Eq. (8), we can obtain the differential scattering efficiency [29]

$$Q_{\text{D}}(\theta, \phi) \triangleq \frac{4}{a^2} \mathbf{F}_{\text{sca}}(\theta, \phi) \cdot \mathbf{F}_{\text{sca}}^*(\theta, \phi) \quad (38)$$

along any radial direction specified by the angles θ and ϕ . The extinction efficiency [38, 29]

$$Q_{\text{ext}} = \frac{4}{k_0 a^2} \text{Im} \{ \mathbf{F}_{\text{sca}}(0, 0) \cdot \hat{\mathbf{x}} \} \quad (39)$$

$$= -\frac{2}{\xi^2} \text{Re} \left\{ \sum_{n=1}^{\infty} [(2n+1)(c_n + e_n)] \right\}, \quad (40)$$

the forward-scattering efficiency [39, 29]

$$Q_{\text{f}} \triangleq Q_{\text{D}}(0, 0) \quad (41)$$

$$= \frac{1}{\xi^2} \left| \sum_{n=1}^{\infty} [(2n+1)(c_n + e_n)] \right|^2, \quad (42)$$

the backscattering efficiency [39]

$$Q_{\text{b}} \triangleq Q_{\text{D}}(\pi, \pi) \quad (43)$$

$$\begin{aligned} &= \frac{1}{\xi^2} \left\{ \left| \sum_{n=1}^{\infty} [(-1)^n (2n+1)(c_n - e_n)] \right|^2 \right. \\ &\quad \left. + 4 \left| \sum_{n=1}^{\infty} [(-1)^n (2n+1)d_n] \right|^2 \right\}, \end{aligned} \quad (44)$$

and the total scattering efficiency [28, 29]

$$Q_{\text{sca}} \triangleq \frac{1}{4\pi} \int_{\phi=0}^{2\pi} \int_{\theta=0}^{\pi} Q_{\text{D}}(\theta, \phi) \sin \theta d\theta d\phi \quad (45)$$

$$= \frac{2}{\xi^2} \sum_{n=1}^{\infty} \{(2n+1) [|c_n|^2 + 2|d_n|^2 + |e_n|^2]\} \quad (46)$$

can be calculated. Let us note that the presence of $\sin \theta$ in the integrand on the right side of Eq. (45) ensures that the magnitudes of Q_{f} and Q_{b} do not affect the magnitude of Q_{sca} .

3 Results and Discussion

The effect of the topologically insulating surface states is seen clearly by setting $\varepsilon_r = \mu_r = 1$; then, $c_n \neq 0$, $d_n \neq 0$, and $e_n \neq 0$ so long as $\gamma \neq 0$. Thus, these surface states by themselves cause scattering,

Intrinsic topological insulators are characterized by $\gamma = \pm \tilde{\alpha}/\eta_0$ [19], where $\tilde{\alpha} = (q_e^2/\hbar c)/4\pi\varepsilon_0$ is the (dimensionless) fine structure constant, $q_e = 1.6 \times 10^{-19}$ C is the quantum of charge, \hbar is the reduced Planck constant, and $c = 1/\sqrt{\varepsilon_0\mu_0}$ is the speed of light in free space. A very thin coating of a magnetic material is often used to realize $\gamma = (2q+1)\tilde{\alpha}/\eta_0$, $q \in \{0, \pm 1, \pm 2, \pm 3, \dots\}$ [19]. Thus, both negative and positive values of γ are possible. The replacement of γ by $-\gamma$ does not affect c_n and e_n , but definitely alters the sign of d_n , as is clear from Eqs. (18)–(21). Concurrently, this replacement does not affect $A_{o1n}^{(3)}$ and $B_{e1n}^{(3)}$, but it does alter the signs of $A_{e1n}^{(3)}$ and $B_{o1n}^{(3)}$, according to Eqs. (37). In other words, the effect of γ on the depolarized scattered fields in planewave scattering is significant. Nevertheless, Q_{ext} and Q_{f} are not directly affected by d_n , whereas Q_{sca} and Q_{b} are not affected by the sign of d_n . Therefore, replacement of γ by $-\gamma$ does not affect any of these four efficiencies. In the remainder of this section, we have confined ourselves to non-negative γ .

When $\gamma = 0$, i.e., in the absence of topologically insulating surface states, Eqs. (18)–(21) yield

$$c_n = -s_n/t_n, \quad (47)$$

$$d_n = 0, \quad (48)$$

$$e_n = -p_n/q_n. \quad (49)$$

Indeed, $-c_n$ and $-e_n$ are then, respectively, equal to the coefficients b_n and a_n of Bohren & Huffman [7, Eqs. (4.53)] for scattering by isotropic dielectric-magnetic spheres.

As γ increases beyond a sufficiently high value, Eqs. (18)–(21) yield

$$c_n \rightarrow -j_n(\xi)/h_n^{(1)}(\xi), \quad (50)$$

$$d_n \rightarrow -1/\eta_0\gamma\xi h_n^{(1)}(\xi)\psi_n^{(3)}(\xi) \rightarrow 0, \quad (51)$$

$$e_n \rightarrow -\psi_n^{(1)}(\xi)/\psi_n^{(3)}(\xi). \quad (52)$$

Thus, at very high values of γ , the right sides of Eqs. (18)–(21) tend towards those of Eqs. (32)–(34), the toroidal-poloidal mixing tends to vanish, and the isotropic dielectric-magnetic sphere with topologically insulating surface states tends to scatter like a PEC sphere.

We carried out a parametric study to numerically assess the effect of γ on scattering. We chose $|\varepsilon_r| \approx 3$, which is reasonable for many materials in the optical regime. We also chose $|\mu_r| \approx 1.3$, which is quite in keeping with ongoing efforts in the area of optical magnetism [40, 41]. Finally, we set $|\gamma| \leq 1000\tilde{\alpha}/\eta_0$, a very wide span for currently researched chalcogenide topological insulators but not inconceivable as the presently infant field of topological insulators grows to encompass mixed materials and new material compositions.

The significance of the limits $\gamma \rightarrow 0$ and $\gamma \rightarrow \infty$ is evident in Fig. 1, wherein Q_{ext} , Q_{sca} , Q_{b} , and Q_{f} are plotted as functions of $\eta_0\gamma/\tilde{\alpha}$ for a nondissipative sphere ($\varepsilon_r = 3$, $\mu_r = 1.3$) of size parameter $\xi = 10$.

Two resonances are evident in these plots for $\eta_0\gamma/\tilde{\alpha} < 400$. As γ increases further, all four efficiencies approach their counterparts for a PEC sphere [39]. Thus, a sphere with topologically insulating surface states becomes perfect electrically conducting in the limit $\gamma \rightarrow \infty$, with Fig. 1 indicating that this transition effectively happens for $\eta_0\gamma/\tilde{\alpha} \approx 1000$.

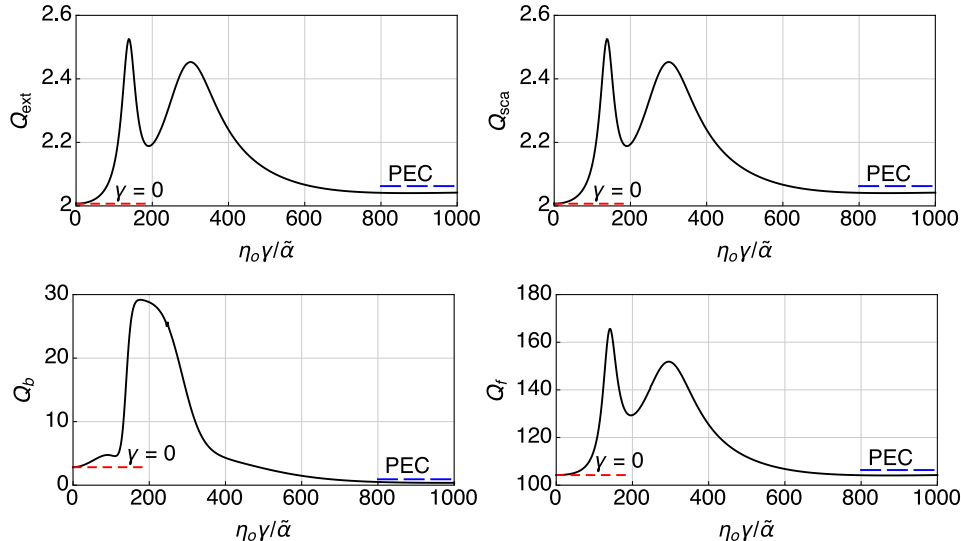


Figure 1: Q_{ext} , Q_{sca} , Q_b , and Q_f as functions of $\eta_0\gamma/\tilde{\alpha}$ for a sphere ($\xi = 10$, $\varepsilon_r = 3$, $\mu_r = 1.3$) embedded in free space. Values for $\gamma = 0$ and a PEC sphere are also indicated.

When the sphere material in Fig. 1 is made dissipative by the addition of positive imaginary parts to ε_r and μ_r , the resonances broaden and eventually disappear. However, as shown in Fig. 2 for $\varepsilon_r = 3 + i0.1$ and $\mu_r = 1.3 + i0.05$ the transition to a PEC sphere still occurs as γ increases.

The data in Figs. 1 and 2 were calculated for spheres of materials that allow planewave propagation with positive phase velocity (PPV); i.e., the phase velocity of a plane wave is co-parallel with the time-averaged Poynting vector [42]. However, if the signs of the real parts of both ε_r and μ_r were to be negative, the phase velocity of a plane wave will be anti-parallel with the time-averaged Poynting vector, so that planewave propagation would occur with negative phase velocity (NPV). Figures 3 and 4 present data for NPV spheres with topologically insulating surface states. Compared to Fig. 1 drawn for $\varepsilon_r = 3$ and $\mu_r = 1.3$, the resonances in Fig. 3 drawn for $\varepsilon_r = -3$ and $\mu_r = -1.3$ are much sharper. However, the incorporation of absorption makes the resonances disappear in Fig. 4 for $\varepsilon_r = -3 + i0.1$ and $\mu_r = -1.3 + i0.05$. As γ increases further, all four efficiencies of an NPV sphere with topologically insulating surface states approach their counterparts for a PEC sphere, just as for a PPV sphere with topologically insulating surface states.

Rayleigh scattering by a homogeneous, isotropic, dielectric-magnetic sphere with topologically insulating surface states requires a comment. Formal expressions for the coefficients c_1 , d_1 , and e_1 can be obtained in the limit $\xi \rightarrow 0$ from Eqs. (18)–(25). But the experimental results of Autore *et al.* [23] clearly show that surface states vanish when the volume is very tiny, indicating that $\gamma = 0$ in the long-wavelength approximation.

4 Concluding Remarks

In the foregoing analysis, the incident, scattered, and internal field phasors were expanded in terms of vector spherical wavefunctions, for electromagnetic scattering by a homogeneous, isotropic, dielectric-magnetic sphere with topologically insulating surface states characterized by a surface admittance γ . Closed-form

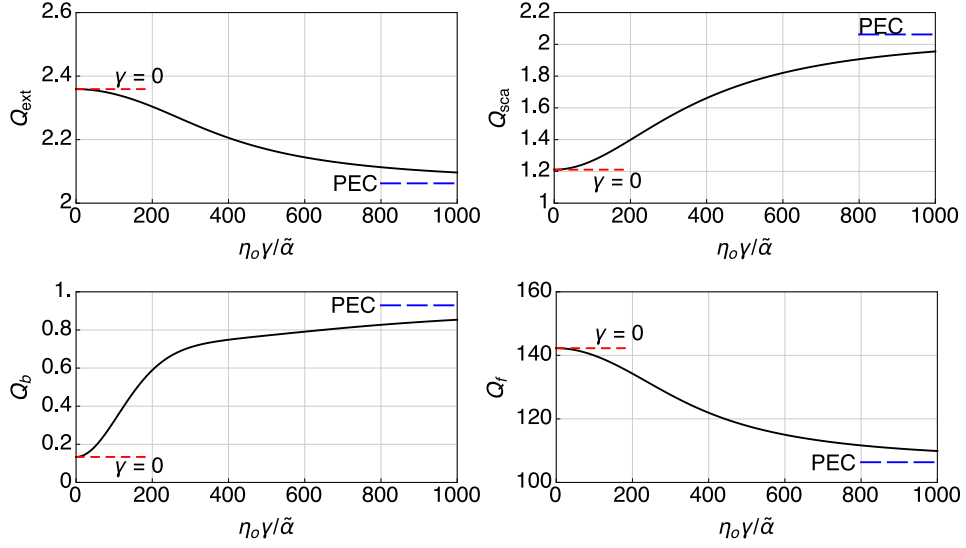


Figure 2: Same as Fig. 1, except that $\varepsilon_r = 3 + i0.1$ and $\mu_r = 1.3 + i0.05$.

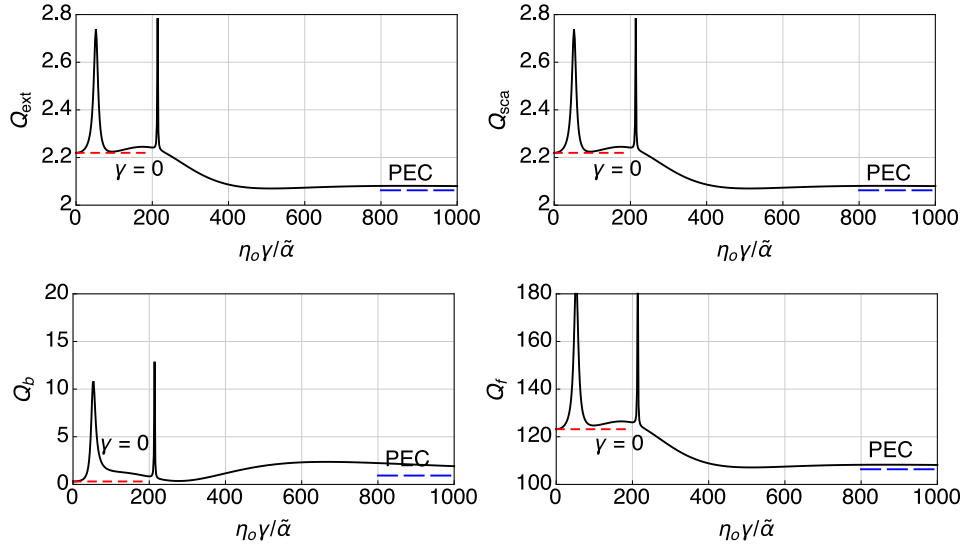


Figure 3: Same as Fig. 1, except that $\varepsilon_r = -3$ and $\mu_r = -1.3$.

expressions were derived for the expansion coefficients of the scattered field phasors in terms of those of the incident field phasors.

Numerical studies demonstrated the presence of resonances due to relatively low values of γ , when the sphere is composed of a nondissipative or weakly dissipative material. Furthermore, the total scattering, extinction, forward scattering, and backscattering efficiencies of the sphere become indistinguishable from those of a perfect electrically conducting sphere for sufficiently large values of γ , regardless of whether

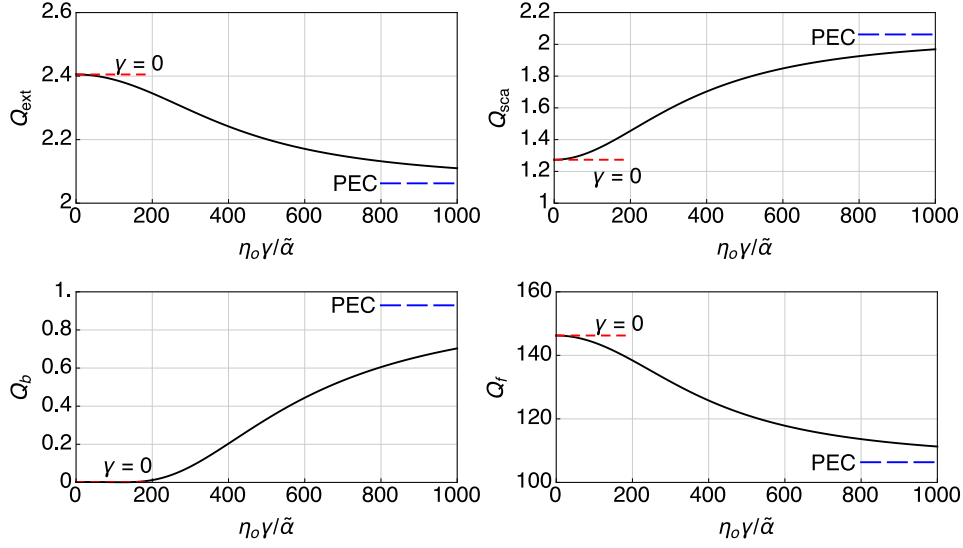


Figure 4: Same as Fig. 3, except that $\varepsilon_r = -3 + i0.1$ and $\mu_r = -1.3 + i0.05$.

the sphere is composed of a dissipative or nondissipative material, and regardless of whether that material supports planewave propagation with positive or negative phase velocity.

Appendix

The vector spherical wavefunctions regular at the origin are defined as [5, 6]

$$\begin{aligned} \mathbf{M}_{\circ_{mn}}^{(1)}(k_0\mathbf{r}) &= \mp \hat{\boldsymbol{\theta}} \frac{mP_n^m(\cos\theta)}{\sin\theta} j_n(k_0r) \begin{Bmatrix} \sin(m\phi) \\ \cos(m\phi) \end{Bmatrix} \\ &\quad - \hat{\boldsymbol{\phi}} \frac{dP_n^m(\cos\theta)}{d\theta} j_n(k_0r) \begin{Bmatrix} \cos(m\phi) \\ \sin(m\phi) \end{Bmatrix} \end{aligned} \quad (53)$$

and

$$\begin{aligned} \mathbf{N}_{\circ_{mn}}^{(1)}(k_0\mathbf{r}) &= \hat{\mathbf{r}} n(n+1) P_n^m(\cos\theta) \frac{j_n(k_0r)}{k_0r} \begin{Bmatrix} \cos(m\phi) \\ \sin(m\phi) \end{Bmatrix} \\ &\quad + \hat{\boldsymbol{\theta}} \frac{dP_n^m(\cos\theta)}{d\theta} \frac{\psi_n^{(1)}(k_0r)}{k_0r} \begin{Bmatrix} \cos(m\phi) \\ \sin(m\phi) \end{Bmatrix} \\ &\quad \mp \hat{\boldsymbol{\phi}} \frac{mP_n^m(\cos\theta)}{\sin\theta} \frac{\psi_n^{(1)}(k_0r)}{k_0r} \begin{Bmatrix} \sin(m\phi) \\ \cos(m\phi) \end{Bmatrix}, \end{aligned} \quad (54)$$

whereas the ones regular at infinity are defined as

$$\begin{aligned} \mathbf{M}_{\circ_{mn}}^{(3)}(k_0\mathbf{r}) &= \mp \hat{\boldsymbol{\theta}} \frac{mP_n^m(\cos\theta)}{\sin\theta} h_n^{(1)}(k_0r) \begin{Bmatrix} \sin(m\phi) \\ \cos(m\phi) \end{Bmatrix} \\ &\quad - \hat{\boldsymbol{\phi}} \frac{dP_n^m(\cos\theta)}{d\theta} h_n^{(1)}(k_0r) \begin{Bmatrix} \cos(m\phi) \\ \sin(m\phi) \end{Bmatrix} \end{aligned} \quad (55)$$

and

$$\begin{aligned}
\mathbf{N}_{\circ_{mn}}^{(3)}(k_0 \mathbf{r}) &= \hat{\mathbf{r}} n(n+1) P_n^m(\cos \theta) \frac{h_n^{(1)}(k_0 r)}{k_0 r} \left\{ \begin{array}{l} \cos(m\phi) \\ \sin(m\phi) \end{array} \right\} \\
&+ \hat{\boldsymbol{\theta}} \frac{dP_n^m(\cos \theta)}{d\theta} \frac{\psi_n^{(3)}(k_0 r)}{k_0 r} \left\{ \begin{array}{l} \cos(m\phi) \\ \sin(m\phi) \end{array} \right\} \\
&\mp \hat{\boldsymbol{\phi}} \frac{mP_n^m(\cos \theta)}{\sin \theta} \frac{\psi_n^{(3)}(k_0 r)}{k_0 r} \left\{ \begin{array}{l} \sin(m\phi) \\ \cos(m\phi) \end{array} \right\}.
\end{aligned} \tag{56}$$

In these expressions,

$$\left. \begin{aligned} \psi_n^{(1)}(w) &= \frac{d}{dw} [w j_n(w)] \\ \psi_n^{(3)}(w) &= \frac{d}{dw} [w h_n^{(1)}(w)] \end{aligned} \right\}, \tag{57}$$

$j_n(\cdot)$ denotes the spherical Bessel function of order n , $h_n^{(1)}(\cdot)$ denotes the spherical Hankel function of the first kind and order n , and $P_n^m(\cdot)$ is the associated Legendre function of order n and degree m .

The angular harmonics used in Eq. (8) are defined as [6]

$$\begin{aligned}
\mathbf{B}_{\circ_{mn}}(\theta, \phi) &= \frac{1}{\sqrt{n(n+1)}} \left[\hat{\boldsymbol{\theta}} \frac{dP_n^m(\cos \theta)}{d\theta} \left\{ \begin{array}{l} \cos(m\phi) \\ \sin(m\phi) \end{array} \right\} \right. \\
&\left. \mp \hat{\boldsymbol{\phi}} \frac{mP_n^m(\cos \theta)}{\sin \theta} \left\{ \begin{array}{l} \sin(m\phi) \\ \cos(m\phi) \end{array} \right\} \right]
\end{aligned} \tag{58}$$

and

$$\begin{aligned}
\mathbf{C}_{\circ_{mn}}(\theta, \phi) &= \frac{1}{\sqrt{n(n+1)}} \left[\mp \hat{\boldsymbol{\theta}} \frac{mP_n^m(\cos \theta)}{\sin \theta} \left\{ \begin{array}{l} \sin(m\phi) \\ \cos(m\phi) \end{array} \right\} \right. \\
&\left. - \hat{\boldsymbol{\phi}} \frac{dP_n^m(\cos \theta)}{d\theta} \left\{ \begin{array}{l} \cos(m\phi) \\ \sin(m\phi) \end{array} \right\} \right].
\end{aligned} \tag{59}$$

The following identities are useful for various derivations:

$$\left. \frac{P_n^1(\cos \theta)}{\sin \theta} \right|_{\theta=0} = \left. \frac{dP_n^1(\cos \theta)}{d\theta} \right|_{\theta=0} = n(n+1)/2, \tag{60}$$

$$\left. \frac{P_n^1(\cos \theta)}{\sin \theta} \right|_{\theta=\pi} = - \left. \frac{dP_n^1(\cos \theta)}{d\theta} \right|_{\theta=\pi} = (-1)^{n+1} n(n+1)/2, \tag{61}$$

$$\begin{aligned}
&\int_0^\pi \left[\frac{mP_n^m(\cos \theta)}{\sin \theta} \frac{dP_{n'}^m(\cos \theta)}{d\theta} + \frac{mP_{n'}^m(\cos \theta)}{\sin \theta} \frac{dP_n^m(\cos \theta)}{d\theta} \right] \\
&\quad \times \sin \theta d\theta = 0,
\end{aligned} \tag{62}$$

and

$$\begin{aligned}
&\int_0^\pi \left[\frac{mP_n^m(\cos \theta)}{\sin \theta} \frac{mP_{n'}^m(\cos \theta)}{\sin \theta} + \frac{dP_n^m(\cos \theta)}{d\theta} \frac{dP_{n'}^m(\cos \theta)}{d\theta} \right] \\
&\quad \times \sin \theta d\theta = \frac{2}{2n+1} \frac{(n+m)! (n+1)!}{(n-m)! (n-1)!} \delta_{nn'}.
\end{aligned} \tag{63}$$

Acknowledgment. AL thanks the Charles Godfrey Binder Endowment at Penn State for ongoing support of his research activities. TGM acknowledges the support of EPSRC grant EP/M018075/1.

References

- [1] N. A. Logan, “Survey of some early studies of the scattering of plane waves by a sphere,” *Proc. IEEE* **53**, 773–785 (1965).
- [2] L. Lorenz, “Lysbevægelsen i og uden for en af plane Lysbølger belyst Kugle,” *Det Kongelige Danske Videnskabernes Selskabs Skrifter* **6**(6), 1–62 (1890).
- [3] L. Lorenz, “Sur la lumière réfléchie et réfractée par une sphère transparente,” in *Oeuvres Scientifiques de L. Lorenz, Revues et annotées par H. Valentine*, Vol. 1, pp. 403–502 (Librairie Lehman & Stage, Copenhagen, 1898). This French translation of Ref. 2 is followed by 27 pages of notes by the translator.
- [4] G. Mie, “Beiträge zur Optik trüber Medien, speziell kolloidaler Metallösungen,” *Ann. Phys. (Leipzig)* **25**, 377–445 (1908).
- [5] J. A. Stratton, *Electromagnetic Theory* (McGraw–Hill, New York, NY, USA, 1941), Chap. 7.
- [6] P. M. Morse and H. Feshbach, *Methods of Theoretical Physics, Vol. II* (McGraw–Hill, New York, NY, USA, 1953), Chap. 13.
- [7] C. F. Bohren and D. R. Huffman, *Absorption and Scattering of Light by Small Particles* (Wiley, New York, NY, USA, 1983), Chap. 4.
- [8] C. F. Bohren, “Light scattering by an optically active sphere,” *Chem. Phys. Lett.* **29**, 458–462 (1974).
- [9] A. D. U. Jafri and A. Lakhtakia, “Scattering of an electromagnetic plane wave by a homogeneous sphere made of an orthorhombic dielectric-magnetic material,” *J. Opt. Soc. Am. A* **31**, 89–100 (2014).
- [10] A. D. U. Jafri and A. Lakhtakia, “Scattering of an electromagnetic plane wave by a homogeneous sphere made of an orthorhombic dielectric-magnetic material: erratum,” *J. Opt. Soc. Am. A* **31**, 2630 (2014).
- [11] H. Masuda, T. Komatsu, and K. Iinoya, “The static electrification of particles in gas-solids pipe flow,” *AIChE J.* **22**, 558–564 (1976).
- [12] S. J. Desch, W. J. Borucki, C. T. Russell, and A. Bar-Nun, “Progress in planetary lightning,” *Rep. Prog. Phys.* **65**, 955–997 (2002).
- [13] M. Sow, E. Crase, J. L. Rajot, R. M. Sankaran, and D. J. Lacks, “Electrification of particles in dust storms: Field measurements during the monsoon period in Niger,” *Atmos. Res.* **102**, 343–350 (2011).
- [14] C. F. Bohren and A. J. Hunt, “Scattering of electromagnetic waves by a charged sphere,” *Can. J. Phys.* **55**, 1930–1935 (1977).
- [15] G. Ya. Slepian, S. A. Maksimenko, A. Lakhtakia, O. Yevtushenko, and A. V. Gusakov, “Electrodynamics of carbon nanotubes: Dynamic conductivity, impedance boundary conditions, and surface wave propagation,” *Phys. Rev. B* **60**, 17136–17149 (1999).
- [16] L. Wei and Y.-N. Wang, “Electromagnetic wave propagation in single-wall carbon nanotubes,” *Phys. Lett. A* **333**, 303–309 (2004).
- [17] A. Moradi, “Guided dispersion characteristics of metallic single-walled carbon nanotubes in the presence of dielectric media,” *Opt. Commun.* **283**, 160–163 (2010).
- [18] M. Z. Hasan and C. L. Kane, “Topological insulators,” *Rev. Mod. Phys.* **82**, 3045–3067 (2010).
- [19] X.-L. Qi, T. L. Hughes, and S.-C. Zhang, “Topological field theory of time-reversal invariant insulators,” *Phys. Rev. B* **78**, 195424 (2008).

- [20] A. Lakhtakia and T. G. Mackay, “Axions, surface states, and the Post constraint in electromagnetics,” *Proc. SPIE* **9558**, 95580C (2015).
- [21] J. F. Nieves and P. B. Pal, “Third electromagnetic constant of an isotropic medium,” *Am. J. Phys.* **62**, 207–216 (1994).
- [22] A. Lakhtakia and W. S. Weiglhofer, “On a constraint on the electromagnetic constitutive relations of nonhomogeneous linear media,” *IMA J. Appl. Math.* **54**, 301–306 (1995).
- [23] M. Autore, F. D’Apuzzo, A. Di Gaspare, V. Giliberti, O. Limaj, P. Roy, M. Brahlek, N. Koirala, S. Oh, F. J. García de Abajo, and S. Lupi, “Plasmon-phonon interactions in topological insulator microrings,” *Adv. Optical Mater.* **3**, 1257–1263 (2015).
- [24] P. J. Wood, “Spherical waves in antenna problems,” *Marconi Rev.* **34**, 149–172 (1971).
- [25] A. Lakhtakia and M. F. Iskander, “Scattering and absorption characteristics of lossy dielectric objects exposed to the near fields of aperture sources,” *IEEE Trans. Antennas Propagat.* **31**, 111–120 (1983).
- [26] S. Chandrasekhar, *Hydrodynamic and Hydromagnetic Stability* (Oxford University Press, New York, NY, USA, 1961).
- [27] P. C. Waterman, “Matrix formulation of electromagnetic scattering,” *Proc. IEEE* **53**, 805–812 (1965).
- [28] P. C. Waterman, “Symmetry, unitarity, and geometry in electromagnetic scattering,” *Phys. Rev. D* **3**, 825–839 (1971).
- [29] D. S. Saxon, “Tensor scattering matrix for the electromagnetic field,” *Phys. Rev.* **100**, 1771–1775 (1955).
- [30] H. C. van de Hulst, *Light Scattering by Small Particles* (Dover Press, New York, NY, USA, 1981), Sec. 6.4.
- [31] H. C. Chen, *Theory of Electromagnetic Waves* (McGraw–Hill, New York, NY, USA, 1983).
- [32] R. J. Garbacz, “Bistatic scattering from a class of lossy dielectric spheres with surface impedance boundary conditions,” *Phys. Rev.* **133**, A14–A16 (1964).
- [33] L. N. Medgyesi-Mitschang and J. M. Putnam, “Integral equation formulations for imperfectly conducting scatterers,” *IEEE Trans. Antennas Propagat.* **33**, 206–214 (1985).
- [34] R. E. Hiatt, T. B. A. Senior, and V. H. Weston, “A study of surface roughness and its effect on the backscattering cross section of spheres,” *Proc. IRE* **48**, 2008–2016 (1960).
- [35] V. H. Weston and R. Hemenger, “High-frequency scattering from a coated sphere,” *J. Res. Nat. Bur. Std. D* **66**, 613–619 (1962).
- [36] L. Ge, D. Han, and J. Zi, “Electromagnetic scattering by spheres of topological insulators,” *Opt. Commun.* **354**, 225–230 (2015).
- [37] A. Lakhtakia and T. G. Mackay, “Classical electromagnetic model of surface states in topological insulators,” *J. Nanophoton.* **10**, 033004 (2016).
- [38] A. T. de Hoop, “On the plane-wave extinction cross-section of an obstacle,” *Appl. Sci. Res. B* **7**, 463–469 (1958).
- [39] J. J. Bowman, T. B. A. Senior, and P. L. E. Uslenghi (Eds.), *Electromagnetic and Acoustic Scattering by Simple Shapes* (North Holland, Amsterdam, The Netherlands, 1969), Chap. 10.

- [40] J. C. Ginn, I. Brener, D. W. Peters, J. R. Wendt, J. O. Stevens, P. F. Hines, L. I. Basilio, L. K. Warne, J. F. Ihlefeld, P. G. Clem, and M. B. Sinclair, “Realizing optical magnetism from dielectric metamaterials,” *Phys. Rev. Lett.* **108**, 097402 (2012).
- [41] S. N. Sheikholeslami, H. Alaeian, A. L. Koh, and J. A. Dionne, “A metafluid exhibiting strong optical magnetism,” *Nano Lett.* **13**, 4137–4141 (2013).
- [42] A. Lakhtakia, M. W. McCall, and W. S. Weiglhofer, “Brief overview of recent developments on negative phase-velocity mediums (*alias* left-handed materials),” *AEÜ Int. J. Electron. Commun.* **56**, 407–410 (2002).